

Densities of Sulfur Hexafluoride and Dinitrogen Monoxide over a Wide Temperature and Pressure Range in the Sub- and Supercritical States

E. Christian Ihmels¹ and Jürgen Gmehling^{1,2}

Received November 5, 2001

Densities of sulfur hexafluoride (SF₆) and dinitrogen monoxide (N₂O) have been measured with a fully computer-controlled high-temperature high-pressure vibrating tube densimeter system in the sub- and supercritical states. The uncertainty in density measurement was estimated to be between ± 0.2 and $\pm 0.3 \text{ kg} \cdot \text{m}^{-3}$ depending on the temperature. With respect to accuracy, reliability, suitability, and time consumption, this system has significant advantages for measuring $P\rho T$ properties in the compressed liquid and supercritical states. The densities were measured for temperatures from 273 to 623 K and at pressures up to 30 MPa for SF₆ (442 data points) and from 273 to 473 K and up to 40 MPa for N₂O (251 data points), which encompassed density ranges between 142.9 and 1778.5 $\text{kg} \cdot \text{m}^{-3}$ for SF₆ and between 124.4 and 1051.1 $\text{kg} \cdot \text{m}^{-3}$ for N₂O. Furthermore, the liquid densities of SF₆ and N₂O were correlated with a new three-dimensional density correlation system (TRIDEN) and the complete set of $P\rho T$ data in the sub- and supercritical states were correlated with a virial-type equation of state. For checking the accuracy and suitability of the vibrating tube densimeter system, the experimental densities of SF₆ were compared with published data and with the results of a reference equation of state.

KEY WORDS: compressed liquid density; compressed supercritical density; correlation; dinitrogen monoxide; sulfur hexafluoride; vibrating tube densimeter.

1. INTRODUCTION

A reliable knowledge of the $P\rho T$ behavior of pure compounds and mixtures is of great importance in many fields of research as well as in industrial

¹ University of Oldenburg, Department of Industrial Chemistry, P.O. Box 2503, D-26111 Oldenburg, Germany.

² To whom correspondence should be addressed. E-mail: Gmehling@tech.chem.uni-oldenburg.de

practice. The densities of fluids as a function of temperature, pressure, and composition are particularly important for the design of industrial plants, pipelines, and pumps. Furthermore, reliable density values are the basis for the development of new correlation equations and improved equations of state. Equations of state and ideal gas heat capacities can be used to calculate phase equilibria and other thermodynamic properties such as enthalpies, entropies, heat capacities, and heats of vaporization at selected conditions (temperature, pressure, and composition). These data are needed for solving material and energy balances required for the design and optimization of chemical processes.

For this purpose a data bank for pure component thermodynamic and transport properties was developed between 1991 and 2001, which is continuously updated [1]. The main objectives of the pure component database are the determination of recommended values, the fitting of recommended correlation parameters, and the development of improved prediction methods for pure component properties. To accomplish this, the database is thoroughly tested, continuously updated, and at the same time data gaps are filled by measurements.

Sulfur hexafluoride and dinitrogen monoxide are two important compounds for very different applications. The uses of sulfur hexafluoride mainly result from its chemical inertness. About 90 to 95% of the sulfur hexafluoride produced is used in electromechanical equipment for insulation. Furthermore, SF_6 is used for insulation in different areas, as for thermoacoustic insulation of windows. A newer application is its use as an inert solvent for chemical reactions in supercritical fluids (SCF). With the measurements presented, the gap in density data for SF_6 at temperatures above 500 K is now covered.

The main uses of dinitrogen monoxide are in medicine as an anesthetic, in the munition and explosive industry as a propellant, and in the food industry as a foaming agent. Up to now, only limited density data for dinitrogen monoxide in the compressed liquid and compressed supercritical states have been published.

For reliable liquid density measurements, vibrating tube densimeters are often applied. The vibrating tube method published by Kratky et al. [2] is well known and has been widely applied for more than 30 years in research, as well as for routine industrial measurements. In this paper the technique is used for the determination of densities in the sub- and supercritical states. In contrast to commercially available vibrating tube densimeters, our prototype can be used over a wider temperature and pressure range. In 1997 the prototype was supplied by "Labor für Meßtechnik Dr. Hans Stabinger" (Graz, Austria). It was designed for temperatures up to 623 K and pressures up to 40 MPa. At first the computer-controlled

apparatus was applied for temperatures up to 523 K and pressures up to 10 MPa for the measurement of liquid densities in the subcritical state [3]. In the second step the environment of the vibrating tube unit was improved, and the range of applicability was extended to higher temperatures and pressures. Measurements of compressed sub- and supercritical densities were performed recently for toluene, carbon dioxide, carbonyl sulfide, and hydrogen sulfide [4]. The measurements for toluene and CO₂ demonstrated the high accuracy, reliability, and suitability of this measurement system. With the computer-controlled measurement system available, it is possible to measure densities over a wide temperature and pressure range in the sub- and supercritical states in a rather short time.

In this work densities in the compressed liquid and supercritical states were measured for SF₆ from 273 to 623 K and at pressures up to 30 MPa (442 data points) and for N₂O from 273 to 473 K and up to 40 MPa (251 data points), which encompassed density ranges between 142.9 and 1778.5 kg·m⁻³ for SF₆ and between 124.4 and 1051.1 kg·m⁻³ for N₂O. The uncertainty in density measurement was estimated to be between ±0.2 and ±0.3 kg·m⁻³ depending on the temperature.

For correlating compressed liquid densities, the widely used Tait equation [5] was employed. This equation needs a reference point for correlating isothermal compressed densities. Typically the Tait equation is used for data below the normal boiling point with the density at atmospheric pressure as reference point. We developed the simple and flexible correlation system TRIDEN for the whole liquid region up to the critical point utilizing the Tait equation [4].

For the correlation of the measured sub- and supercritical data, a virial-type equation of state was employed. With the correlation equations developed, the data can be described within the experimental uncertainties.

2. EXPERIMENTAL

A density measurement with a vibrating tube is based on the dependence between the period of oscillation of an unilaterally fixed U-tube and its mass. This mass consists of the U-tube material and the mass of the fluid filled into the U-tube. The behavior of the vibrating tube can be described by a simple mathematical-physical model of an undamped spring-mass system [2]. The characteristic period of oscillation τ (μ s) of this model is described by the following equation,

$$\tau = 2\pi \sqrt{\frac{m_0 + V\rho}{D}} \quad (1)$$

where m_0 is the mass of the empty U-tube (in kg), V is the volume of the vibrating tube (in m^3), ρ is the density (in $\text{kg}\cdot\text{m}^{-3}$), and D is the spring constant (in $\text{N}\cdot\text{m}^{-1}$).

Rearrangement of the equation and substitution of the mechanical constants lead to the classical equation for vibrating tube densimeters:

$$\rho = A\tau^2 - B \quad (2)$$

The parameters A and B can be determined by calibration measuring the period of oscillation of at least two substances of known density. Unfortunately, the parameters A and B are highly temperature and also pressure dependent. Therefore, the parameters must be determined for each temperature and pressure independently, or as applied in this work, the classical equation (2) must be extended with temperature- and pressure-dependent terms. For measurements over such a large temperature range as in this work (273 to 623 K) and up to 40 MPa, an extended calibration equation (3) with 14 significant parameters is employed. Using more than 750 data points (measurements on water, butane, and vacuum) for calibration, over-fitting is prevented.

2.1. Apparatus

A schematic of the density measurement system is shown in Fig. 1. The high-pressure high-temperature vibrating tube densimeter (DMA-HDT) is the essential part of the computer-controlled system. The DMA-HDT system consists of the measurement cell and a modified DMA 5000 control unit. The measurement cell contains the vibrating tube (Hastelloy C-276), the sensor and excitation coils, a thermostat with cooling circuit (e.g., for air or water cooling), and two temperature sensors. The period of oscillation measurement and the temperature control is implemented within the DMA-HDT control unit. This control unit is connected to a PC via a serial port (RS232). A target temperature can be sent to the control unit, and the temperature and the period of oscillation are controlled by the PC.

The vibrating tube unit is connected with high pressure tubing and valves (HIP 30,000 psi series from HIP, Erie, Pennsylvania, U.S.A.) to a variable volume cell (dosage pump Type 2200-802 from Ruska, Houston, Texas, U.S.A.). The piston of the variable volume cell can be moved by a stepping motor (Model RSH 125-200-10 from Phytron, Groebenzell, Germany) connected to a power/control unit (Model ix alpha-c from Phytron) which is also connected to a PC via a serial port.

For the pressure measurement two pressure transducers (Model PDCR 911 up to 20 MPa, Model PDCR 922 up to 60 MPa, both from

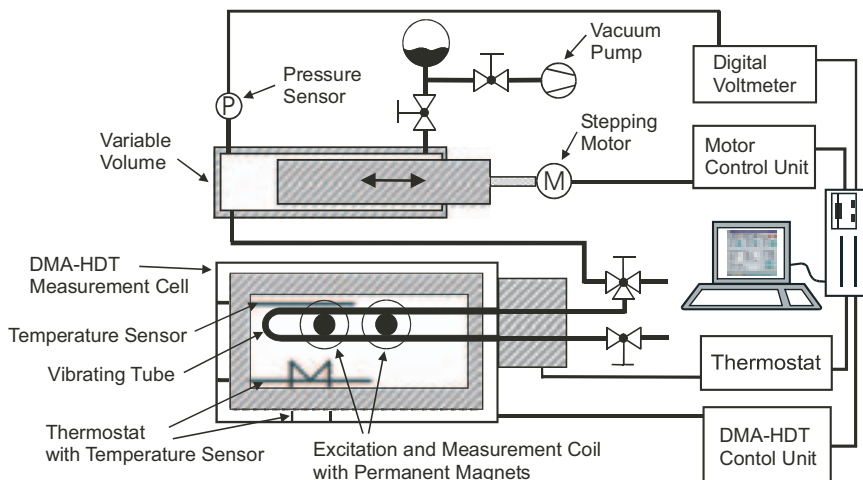


Fig. 1. Schematic of the computer-controlled density measurement unit.

Druck, Leicester, England) are used. A multimeter (Model 2000 from Keithley, Cleveland, Ohio, U.S.A.) with a serial port is employed for the transformation of the pressure transducer measurement signal.

To prevent undesirable temperature- and resulting density-gradients in the vibrating tube region of the apparatus, heating (aluminum-block with heating cartridges) was provided around the supply pipes next to the vibrating tube. For this heating a thermostat unit (Model 2416 from Eurotherm, Heppenheim, Germany) is connected to the PC. For measurements at temperatures from 273 up to 313 K, a thermostat (Model RC GCP Edition 2000 from Lauda, Lauda-Koenigshofen, Germany) with a water-ethanol mixture is attached to the mentioned cooling circuit of the vibrating tube unit. For evacuating the whole apparatus a vacuum pump (Model RZ 2 from Vacuubrand, Wertheim, Germany, with sensor Thermovac TM 20 from Leybold, Cologne, Germany) is employed.

The vibrating tube unit can be disconnected from the variable volume cell with the use of a three-way valve. In this mode density measurements at atmospheric pressure are possible using small amounts of sample. Density measurements at atmospheric pressure were already presented by Ihmels et al. [3].

The whole apparatus can be controlled with the developed control program “Densitas per Motum—Density Measurement“ [4]. With this software fully automated temperature-pressure measurement programs can be implemented.

2.2. Measurement Range, Accuracy, and Calibration

The Pt100 temperature sensors installed show a resolution of ± 3 mK and an accuracy of ± 30 mK, while the thermostat has a stability of ± 20 mK. The period of oscillation is measured with a resolution of 1 ns and shows values between 2200 and 2600 μs depending on density, temperature, and pressure. The observed reproducibility of the density measurements at atmospheric pressure and temperatures from 298 up to 373 K is within ± 0.05 $\text{kg}\cdot\text{m}^{-3}$. At higher pressures and temperatures, hysteresis effects in the vibrating tube material limit the reproducibility to ± 0.1 $\text{kg}\cdot\text{m}^{-3}$. The pressure sensors are designed for pressures up to 20 and 60 MPa, and the accuracy after calibration with a dead-weight pressure gauge was estimated to be better than ± 2 and ± 6 kPa, respectively. The accuracy in the density measurement depends on the accuracy of the pressure, temperature, and period of oscillation measurements as well as on the purity of the reference substances and accuracy of the reference densities used.

For the calibration the periods of oscillation of the two reference substances (water and butane) and the period of oscillation in vacuum were used. Water was measured in the temperature range from 278 to 623 K and butane between 273 and 428 K (both in 5 K steps). Both substances were measured at pressures from approximately 0.3 MPa above the vapor pressure up to 40 MPa (in 5 MPa steps). Moreover, the vacuum signal (density = 0 $\text{kg}\cdot\text{m}^{-3}$) was measured between 273 and 623 K. Then the parameters of a 14-parameter calibration equation [Eq. (3)] were fitted to the calibration points (temperature, pressure, and period of oscillation) to the reference densities calculated using the reference equation of state from Pruß and Wagner [6, 7] for water and the reference equation from Younglove and Ely [8] for butane and the zero density (in vacuum) by linear regression.

The following equation was used to determine the densities from the measured period of oscillation at a given temperature T (K) and pressure P (MPa).

$$\rho = A\tau^2 - B$$

$$\text{with } A = \sum_i a_i T^i + \sum_j b_j P^j + cTP \quad \text{and} \quad B = \sum_i d_i T^i + \sum_j e_j P^j + fTP$$

$$\text{with } i = 0, 1, 2, 3 \quad \text{and} \quad j = 1, 2 \quad (3)$$

For density measurements at atmospheric pressure in the temperature range between 298 and 373 K, a maximum error of ± 0.1 $\text{kg}\cdot\text{m}^{-3}$ is

obtained. For pressures up to 40 MPa and temperatures from 273 up to 623 K, the total error in the density measurement is estimated to be $\pm 0.3 \text{ kg} \cdot \text{m}^{-3}$. In the moderate range between 298 and 523 K the maximum error is estimated to be within $\pm 0.2 \text{ kg} \cdot \text{m}^{-3}$. For the measured liquid densities between 400 and $1500 \text{ kg} \cdot \text{m}^{-3}$, this leads to relative errors between ± 0.075 and $\pm 0.02\%$. In the compressed supercritical region only densities above $100 \text{ kg} \cdot \text{m}^{-3}$ were measured. This leads to maximum relative errors of $\pm 0.3\%$. Because of the strong pressure dependence of the densities near the critical point, higher deviations result in this region. With an uncertainty of about $\pm 6 \text{ kPa}$ in pressure, a maximum error in density of about $\pm 0.5\%$ is estimated for the supercritical region near the critical pressure, and in the region near the critical point, an error of about $\pm 2\%$ is estimated.

2.3. Experimental Procedure

For the high pressure density measurements carried out, 75 to 100 cm^3 of liquid or compressed gas are required. The compressed gases were injected into the evacuated apparatus from a gas cylinder. The measurement programs run from the minimum temperature to the maximum temperature in defined steps. At each temperature a preset pressure program is executed from minimum to maximum pressure in defined steps. The control program sets the target temperature and pressure and waits for a defined time until equilibrium system conditions have been attained. After recording and storing the measured values with a specified number of repetitions, the program starts the next measurement. After the maximum pressure has been reached, the pressure is reduced to the minimum pressure and the next temperature is set.

At the end of the measurement program, the temperature and pressure are decreased to the stand-by values.

A temperature-pressure program between 273 and 623 K and at pressures up to 40 MPa with approximately 600 measurement points can be realized within one week. Atmospheric pressure measurements in a temperature range between 308 and 498 K with 40 experimental data require two days.

2.4. Chemicals

The compounds used for the measurements are sulfur hexafluoride (SF_6 , $M = 146.05 \text{ g} \cdot \text{mol}^{-1}$, CAS-RN 2551-62-4) and dinitrogen monoxide (N_2O , $M = 44.01 \text{ g} \cdot \text{mol}^{-1}$, CAS-RN 10024-97-2). Sulfur hexafluoride (purity 99.9%) and dinitrogen monoxide (purity 99.5%) were both

obtained from Messer Griesheim (Krefeld, Germany). The purities were checked by gas chromatography.

3. RESULTS AND DISCUSSION

In this work the densities of SF_6 and N_2O in the sub- and supercritical states were measured. The measurements of SF_6 from 273 to 623 K and from 3 up to 30 MPa (442 data points) and of N_2O from 273 to 473 K and from 6 up to 40 MPa (251 data points) are presented in Figs. 2 and 3 and in Tables I and II.

Densities of SF_6 in the liquid and supercritical state have already been measured by other researchers up to temperatures around 500 K [1]. With the new measurements for SF_6 the temperature range was extended up to 623 K. The densities of SF_6 below 500 K can be used as further evidence for the accuracy and suitability of the apparatus for the measurements of densities at sub- and supercritical conditions. Therefore, these data were compared with the calculated values using the IUPAC interim reference equation of state for SF_6 from de Reuck et al. [9]. In Fig. 4 the deviations between the experimental densities measured in this work and the results of the equation of state are presented. The pressures of the data points and the temperature limit of the equation of state at 525 K are marked in the temperature-density deviation plot. The deviations are within $\pm 0.2\%$ in the liquid and moderate supercritical range and reach $\pm 0.4\%$ at 525 K. The higher deviations above the EOS limit of 525 K are expected, but with

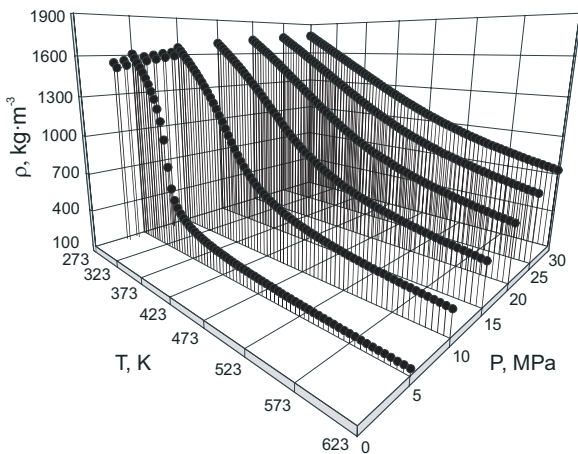


Fig. 2. Densities of sulfur hexafluoride (SF_6) at temperatures between 273 and 623 K and at pressures up to 30 MPa.

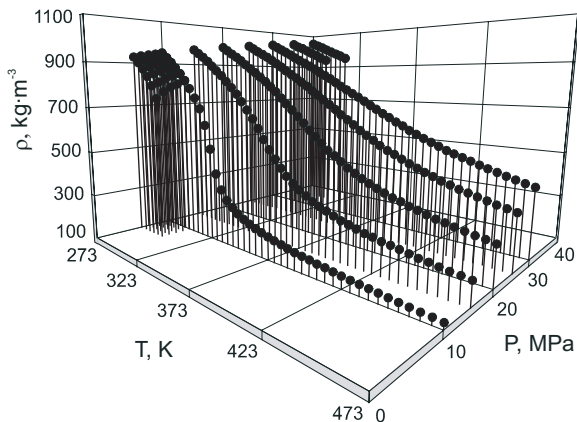


Fig. 3. Densities of dinitrogen monoxide (N_2O) at temperatures between 273 and 473 K and at pressures between 6 and 40 MPa.

values less than $\pm 1\%$ that are very reasonable. De Reuck et al. estimated an uncertainty of 0.1% in density for their equation of state. Therefore, in Fig. 5 the deviations between our experimental densities are shown together with densities published by other authors and the results of the equation of state from de Reuck et al. [9]. From about 20 references for compressed densities of SF_6 stored in our data bank [1], some newer and some older published data covering the temperature and pressure range of our measurements were selected [10–15]. The pressure range of the compared data

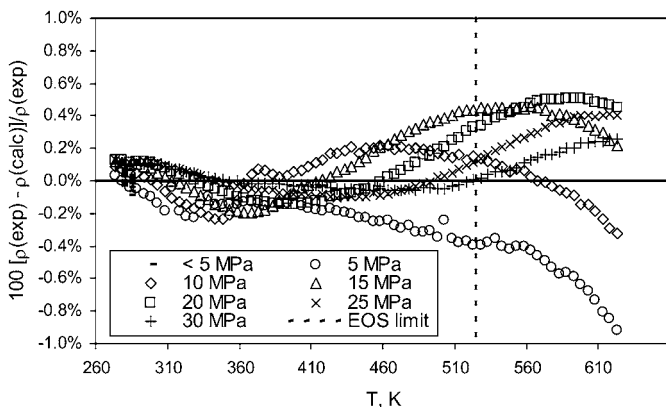


Fig. 4. Relative deviations between the experimental densities measured in this work and the equation of state for sulfur hexafluoride from de Reuck et al. [9] ($T_c = 318.7 \text{ K}$, $P_c = 3.76 \text{ MPa}$).

Table I. Experimental Densities of Sulfur Hexafluoride (SF₆) in the Compressed Liquid and Supercritical States

<i>T</i> (K)	<i>P</i> (MPa)	ρ (kg · m ⁻³)
278.40	2.953	1545.37
278.39	3.953	1560.41
278.39	4.977	1574.38
278.38	5.978	1586.93
278.38	6.981	1598.57
278.38	7.979	1609.46
278.38	8.979	1619.65
278.38	9.979	1629.28
283.37	3.024	1507.86
283.37	3.977	1524.60
283.37	4.977	1540.35
283.37	5.978	1554.63
283.37	6.978	1567.70
283.37	7.978	1579.81
283.37	8.978	1591.11
283.37	9.979	1601.69
273.38	5.024	1607.26
273.38	9.979	1656.08
273.38	14.981	1694.63
273.38	19.982	1726.62
273.38	24.984	1754.24
273.38	29.983	1778.54
278.37	5.024	1575.05
278.37	9.979	1629.34
278.37	14.981	1671.02
278.37	19.982	1705.14
278.37	24.984	1734.32
278.37	29.987	1759.89
283.37	5.024	1541.11
283.37	9.980	1601.73
283.37	14.979	1646.95
283.37	19.983	1683.37
283.37	24.983	1714.15
283.37	29.985	1741.03
288.35	5.024	1505.67
288.35	9.978	1573.83
288.35	14.979	1622.96
288.35	19.981	1661.77
288.35	24.983	1694.33
288.35	29.990	1722.52
293.35	5.019	1467.20
293.35	9.978	1544.67
293.35	14.979	1598.20
293.36	19.982	1639.75

Table I. (Continued)

T (K)	P (MPa)	ρ ($\text{kg} \cdot \text{m}^{-3}$)
293.36	24.982	1674.13
293.36	29.986	1703.67
298.33	5.024	1426.20
298.33	9.979	1514.83
298.33	14.981	1573.24
298.33	19.983	1617.62
298.33	24.985	1654.03
298.34	29.986	1685.04
303.32	5.024	1380.58
303.32	9.978	1483.58
303.32	14.981	1547.37
303.32	19.983	1595.07
303.32	24.984	1633.58
303.32	29.987	1666.10
308.31	5.024	1329.23
308.31	9.979	1450.95
308.31	14.980	1521.08
308.31	19.981	1572.18
308.31	24.982	1612.90
308.31	29.984	1647.10
313.28	5.024	1272.48
313.29	9.979	1416.98
313.30	14.981	1494.31
313.30	19.983	1549.13
313.30	24.984	1592.22
313.30	29.984	1628.05
318.29	5.024	1199.40
318.30	9.992	1381.94
318.30	14.989	1467.15
318.31	19.982	1525.75
318.31	24.981	1571.33
318.31	29.986	1608.98
323.30	5.024	1106.79
323.30	9.979	1344.66
323.30	14.980	1439.10
323.30	19.982	1502.14
323.30	24.984	1550.43
323.30	29.985	1589.84
328.29	5.024	969.83
328.30	9.979	1305.76
328.30	14.980	1410.60
328.30	19.983	1478.29
328.30	24.982	1529.32
328.30	29.985	1570.62
333.29	5.024	758.52

Table I. (Continued)

T (K)	P (MPa)	ρ (kg · m ⁻³)
333.29	9.979	1264.90
333.29	14.980	1381.50
333.29	19.981	1454.16
333.29	24.983	1508.16
333.29	29.986	1551.40
338.28	5.024	592.27
338.28	9.978	1221.96
338.28	14.979	1351.83
338.28	19.981	1429.78
338.28	24.983	1486.76
338.28	29.984	1532.11
343.27	5.024	506.92
343.27	9.979	1176.91
343.27	14.981	1321.57
343.27	19.984	1405.32
343.27	24.983	1465.40
343.27	29.983	1512.85
348.26	5.024	455.27
348.27	9.979	1129.93
348.27	14.979	1290.92
348.27	19.982	1380.55
348.27	24.982	1443.95
348.27	29.985	1493.55
353.26	5.024	419.15
353.26	9.992	1081.86
353.26	14.981	1259.72
353.27	19.978	1355.61
353.27	24.984	1422.48
353.27	29.985	1474.21
358.26	5.024	391.88
358.26	9.982	1031.70
358.26	14.980	1228.15
358.26	19.981	1330.60
358.26	24.983	1400.93
358.26	29.983	1455.04
363.25	5.024	370.03
363.26	9.977	981.45
363.26	14.981	1196.29
363.26	19.982	1305.54
363.26	24.984	1379.44
363.26	29.987	1435.76
368.25	5.024	351.98
368.25	9.978	931.89
368.25	14.980	1164.31

Table I. (Continued)

T (K)	P (MPa)	ρ (kg·m ⁻³)
368.25	19.984	1280.33
368.25	24.984	1357.99
368.25	29.984	1416.61
373.24	5.024	336.57
373.24	9.978	884.01
373.24	14.979	1132.30
373.24	19.981	1255.27
373.24	24.983	1336.49
373.24	29.984	1397.52
378.24	5.025	323.24
378.24	9.978	838.62
378.24	14.980	1100.37
378.24	19.981	1230.16
378.24	24.983	1315.16
378.24	29.984	1378.53
383.23	5.024	311.53
383.23	9.978	796.26
383.23	14.980	1068.76
383.24	19.985	1205.21
383.24	25.022	1294.49
383.24	29.985	1359.54
388.23	5.024	301.04
388.23	9.980	757.47
388.23	14.980	1037.66
388.23	19.980	1180.37
388.24	24.980	1272.60
388.24	29.984	1340.70
393.23	5.024	291.61
393.23	9.978	721.89
393.23	14.979	1006.88
393.23	19.980	1155.70
393.23	24.982	1251.56
393.23	29.985	1321.99
398.23	5.018	282.70
398.23	9.978	689.94
398.23	14.981	977.24
398.23	19.982	1131.44
398.23	24.982	1230.76
398.23	29.985	1303.33
403.22	5.024	275.19
403.22	9.978	660.84
403.22	14.981	948.37
403.23	19.982	1107.43
403.23	24.984	1210.10

Table I. (Continued)

T (K)	P (MPa)	ρ (kg·m ⁻³)
403.23	29.985	1284.97
408.22	5.024	267.94
408.22	9.978	634.57
408.22	14.978	920.42
408.22	19.982	1083.85
408.22	24.984	1189.70
408.22	29.986	1266.74
413.21	5.024	261.26
413.21	9.978	610.82
413.21	14.978	893.60
413.21	19.981	1060.76
413.21	24.984	1169.53
413.21	29.984	1248.76
418.21	5.024	255.02
418.21	9.978	589.15
418.21	14.981	868.04
418.22	19.992	1038.21
418.23	25.022	1150.50
418.22	29.984	1230.81
423.21	5.024	249.25
423.21	9.978	569.44
423.21	14.980	843.42
423.21	19.982	1016.10
423.21	24.981	1130.06
423.22	29.983	1213.14
428.21	5.024	243.79
428.21	9.978	551.28
428.21	14.979	820.15
428.21	19.981	994.54
428.21	24.985	1110.85
428.21	29.986	1195.78
433.21	5.024	238.70
433.21	9.978	534.64
433.21	14.978	797.89
433.21	19.982	973.53
433.21	24.982	1091.98
433.21	29.985	1178.66
438.20	5.024	233.86
438.21	9.977	519.33
438.21	14.980	776.89
438.21	19.981	953.16
438.21	24.984	1073.52
438.21	29.985	1161.77
443.20	5.024	229.28

Table I. (Continued)

T (K)	P (MPa)	ρ (kg·m ⁻³)
443.20	9.978	505.00
443.20	14.979	756.92
443.20	19.980	933.41
443.20	24.982	1055.37
443.20	29.984	1145.22
448.20	5.024	224.94
448.20	9.977	491.87
448.20	14.979	737.98
448.20	19.980	914.30
448.20	24.983	1037.63
448.20	29.983	1128.86
453.19	5.024	220.83
453.19	9.978	479.62
453.20	14.981	720.17
453.21	20.011	896.74
453.21	25.019	1021.23
453.20	29.984	1112.81
458.20	5.024	216.92
458.20	9.979	468.27
458.20	14.980	703.11
458.20	19.981	878.10
458.20	24.983	1003.38
458.20	29.982	1097.11
463.20	5.024	213.21
463.20	9.979	457.49
463.20	14.980	686.91
463.20	19.982	861.04
463.20	24.983	986.95
463.20	29.986	1081.67
468.20	5.024	209.63
468.20	9.979	447.27
468.20	14.980	671.64
468.20	19.981	844.33
468.20	24.982	970.92
468.20	29.984	1066.47
473.20	5.024	206.19
473.20	9.977	437.77
473.20	14.980	657.06
473.20	19.980	828.33
473.20	24.980	955.20
473.20	29.982	1051.65
478.19	5.022	202.91
478.19	9.978	428.76
478.19	14.979	643.29

Table I. (Continued)

T (K)	P (MPa)	ρ ($\text{kg} \cdot \text{m}^{-3}$)
478.19	19.981	812.94
478.19	24.983	940.04
478.19	29.984	1037.23
483.19	5.024	199.80
483.19	9.978	420.31
483.19	14.980	630.16
483.19	19.980	798.13
483.19	24.983	925.23
483.19	29.985	1022.97
488.19	5.024	196.80
488.19	9.979	412.28
488.19	14.979	617.64
488.20	20.024	785.25
488.20	24.984	910.86
488.19	29.985	1009.11
493.19	5.025	193.96
493.19	9.980	404.68
493.20	14.980	605.74
493.20	19.996	770.39
493.20	24.989	896.93
493.20	29.981	995.42
498.20	5.025	191.11
498.20	9.981	397.39
498.20	14.978	594.26
498.20	19.980	756.74
498.20	24.982	883.32
498.20	29.986	982.10
503.20	5.015	188.25
503.20	9.979	390.32
503.20	14.980	583.47
503.20	19.980	743.91
503.20	24.981	869.97
503.20	29.986	969.10
508.19	5.024	185.83
508.19	9.979	383.71
508.19	14.980	573.10
508.19	19.979	731.66
508.19	24.982	857.17
508.19	29.985	956.47
513.19	5.024	183.30
513.19	9.978	377.44
513.19	14.979	563.25
513.19	19.981	719.80
513.19	24.982	844.69

Table I. (Continued)

T (K)	P (MPa)	ρ ($\text{kg} \cdot \text{m}^{-3}$)
513.19	29.984	944.06
518.19	5.024	180.89
518.19	9.979	371.33
518.19	14.978	553.73
518.19	19.981	708.43
518.19	24.983	832.64
518.19	29.983	931.97
523.19	5.024	178.55
523.19	9.978	365.59
523.19	14.981	544.66
523.19	19.980	697.38
523.19	24.983	820.86
523.19	29.984	920.21
528.19	5.024	176.30
528.19	9.977	359.98
528.19	14.984	536.04
528.19	19.980	686.62
528.19	24.982	809.40
528.19	29.983	908.66
533.19	5.024	174.15
533.19	9.978	354.61
533.19	14.981	527.48
533.19	19.980	676.37
533.19	24.983	798.34
533.19	29.984	897.51
538.19	5.021	171.95
538.19	9.979	349.49
538.19	14.981	519.43
538.19	19.980	666.41
538.19	24.983	787.61
538.19	29.982	886.50
543.18	5.024	169.93
543.19	9.978	344.48
543.19	14.981	511.65
543.19	19.981	656.78
543.19	24.983	777.12
543.19	29.986	875.69
548.19	5.024	167.92
548.19	9.979	339.65
548.19	14.980	504.05
548.19	19.982	647.51
548.19	24.983	766.91
548.19	29.984	865.16
553.18	5.024	166.01

Table I. (Continued)

T (K)	P (MPa)	ρ (kg·m ⁻³)
553.18	9.977	335.07
553.18	14.979	496.88
553.18	19.980	638.53
553.18	24.982	757.06
553.18	29.983	854.95
558.18	5.024	164.11
558.18	9.979	330.70
558.19	14.980	489.93
558.19	19.986	629.93
558.19	24.989	747.50
558.19	29.989	845.18
563.19	5.024	162.25
563.19	9.989	326.62
563.19	14.983	483.38
563.19	19.980	621.43
563.19	24.983	738.03
563.19	29.984	835.38
568.19	5.024	160.41
568.19	9.984	322.24
568.19	14.981	476.80
568.19	19.981	613.28
568.19	24.983	728.88
568.19	29.980	825.73
573.19	5.024	158.64
573.19	9.983	318.19
573.19	14.980	470.45
573.20	19.980	605.32
573.20	24.980	720.04
573.20	29.983	816.50
578.20	5.024	156.88
578.20	9.978	314.09
578.20	14.979	464.24
578.20	19.982	597.64
578.20	24.978	711.37
578.20	29.985	807.36
583.19	5.024	155.18
583.19	9.978	310.29
583.19	14.979	458.40
583.19	19.981	590.16
583.19	24.983	703.02
583.19	29.984	798.46
588.19	5.024	153.57
588.20	9.977	306.56
588.19	14.979	452.71

Table I. (Continued)

T (K)	P (MPa)	ρ (kg·m ⁻³)
588.20	19.979	582.87
588.20	24.982	694.82
588.19	29.985	789.89
593.19	5.024	151.99
593.19	9.979	303.05
593.19	14.980	447.17
593.19	19.981	575.89
593.19	24.982	686.90
593.19	29.985	781.29
598.19	5.024	150.39
598.19	9.978	299.44
598.20	14.979	441.75
598.20	19.980	569.02
598.20	24.983	679.11
598.20	29.982	773.10
603.20	5.024	148.84
603.20	9.978	296.13
603.20	14.980	436.51
603.20	19.982	562.38
603.20	24.983	671.49
603.20	29.984	764.98
608.19	5.024	147.30
608.20	9.978	292.76
608.20	14.980	431.39
608.20	19.980	555.78
608.20	24.983	664.02
608.20	29.985	757.01
613.20	5.024	145.78
613.20	9.978	289.48
613.20	14.979	426.46
613.20	19.979	549.46
613.20	24.983	656.81
613.20	29.984	749.22
618.20	5.024	144.34
618.20	9.978	286.30
618.20	14.979	421.54
618.20	19.981	543.36
618.20	24.982	649.79
618.20	29.983	741.65
623.19	5.024	142.86
623.20	9.978	283.21
623.20	14.981	416.84
623.20	19.980	537.33
623.20	24.984	642.86
623.20	29.984	734.17

Table II. Experimental Densities of Dinitrogen Monoxide (N_2O) in the Compressed Liquid and Supercritical States

T (K)	P (MPa)	ρ ($\text{kg} \cdot \text{m}^{-3}$)
273.39	5.976	926.40
273.39	6.978	932.94
273.39	7.977	938.99
273.39	8.979	944.74
273.38	9.980	950.20
278.37	6.023	899.94
278.37	6.977	907.32
278.37	7.977	914.53
278.37	8.978	921.21
278.37	9.979	927.49
283.34	6.025	870.20
283.34	6.977	879.35
283.35	7.978	888.06
283.35	8.976	896.01
283.35	9.978	903.37
288.32	6.024	836.24
288.33	6.977	848.09
288.33	7.978	858.98
288.33	8.979	868.69
288.33	9.979	877.42
293.31	6.024	795.16
293.31	6.977	811.81
293.31	7.977	826.13
293.31	8.977	838.32
293.31	9.979	849.06
298.30	6.024	739.68
298.31	6.996	767.41
298.31	8.024	788.49
298.31	8.976	803.96
298.30	9.980	817.63
273.39	9.978	950.03
273.38	14.983	973.74
273.38	19.985	993.38
273.38	24.986	1010.29
273.38	29.984	1025.28
273.38	34.990	1038.77
273.38	39.992	1051.07
278.37	10.023	927.64
278.37	14.982	954.06
278.37	19.985	975.65

Table II. (Continued)

T (K)	P (MPa)	ρ ($\text{kg} \cdot \text{m}^{-3}$)
278.37	24.985	993.97
278.37	29.988	1010.03
278.37	34.992	1024.34
278.37	39.985	1037.32
283.35	10.023	903.49
283.35	14.982	933.54
283.36	19.982	957.42
283.36	24.986	977.34
283.36	29.985	994.60
283.36	34.990	1009.84
283.36	39.983	1023.54
288.34	10.023	877.55
288.34	14.981	912.20
288.34	19.985	938.66
288.34	24.989	960.37
288.34	29.987	978.89
288.34	34.991	995.16
288.34	39.980	1009.63
293.32	10.023	849.22
293.32	14.982	889.68
293.32	19.982	919.28
293.32	24.987	942.98
293.32	29.989	962.88
293.32	34.994	980.24
293.32	39.984	995.63
298.31	10.023	817.72
298.31	14.980	865.87
298.31	19.984	899.14
298.31	24.989	925.11
298.31	29.988	946.60
298.32	34.984	965.12
298.32	40.017	981.52
303.31	10.021	781.78
303.31	14.981	840.59
303.32	19.983	878.24
303.32	24.984	906.74
303.32	29.986	930.00
303.31	34.988	949.77
303.31	39.978	967.07
308.31	10.022	740.35
308.32	14.980	813.83
308.32	19.983	856.83

Table II. (Continued)

T (K)	P (MPa)	ρ ($\text{kg} \cdot \text{m}^{-3}$)
308.32	24.987	888.22
308.32	29.986	913.35
308.33	34.995	934.48
308.33	39.981	952.79
313.28	10.023	692.58
313.30	14.983	785.60
313.30	19.983	834.96
313.30	24.987	869.61
313.30	29.988	896.72
318.30	10.023	618.84
318.30	14.981	754.69
318.31	19.983	811.81
318.31	24.985	850.15
318.31	29.988	879.51
323.30	10.024	515.88
323.30	14.982	720.92
323.30	19.983	787.56
323.30	24.984	830.09
323.30	29.988	861.97
328.29	10.018	405.91
328.29	14.981	683.91
328.29	19.986	762.20
328.29	24.986	809.43
328.29	29.988	844.03
333.28	10.024	339.25
333.28	14.981	643.75
333.28	19.984	735.79
333.29	24.985	788.34
333.29	29.986	825.88
338.28	10.024	299.50
338.28	15.023	602.09
338.28	19.982	708.41
338.28	24.985	766.75
338.28	29.986	807.43
343.27	10.023	272.76
343.28	14.982	556.39
343.28	19.981	680.26
343.28	24.984	744.92
343.28	29.987	788.87
348.27	10.023	253.01
348.27	14.979	512.71
348.27	19.981	651.46

Table II. (Continued)

T (K)	P (MPa)	ρ ($\text{kg} \cdot \text{m}^{-3}$)
348.27	24.985	722.71
348.27	29.988	770.24
353.26	10.023	237.62
353.27	14.977	472.26
353.27	19.981	622.29
353.27	24.982	700.20
353.27	29.986	751.29
358.26	10.024	225.05
358.26	14.977	436.51
358.26	19.981	593.18
358.26	24.984	677.59
358.27	29.985	732.29
363.26	10.021	214.42
363.26	14.980	405.83
363.26	19.982	564.78
363.26	24.983	655.03
363.26	29.986	713.39
368.25	10.023	205.42
368.25	14.979	379.82
368.25	19.982	537.38
368.25	24.987	632.65
368.25	29.986	694.45
373.24	10.023	197.49
373.24	14.980	357.67
373.24	19.983	511.34
373.24	24.985	610.57
373.24	29.989	675.72
378.24	10.024	190.44
378.24	14.980	338.80
378.24	19.984	487.08
378.24	24.982	588.95
378.24	29.988	657.05
383.23	10.023	184.17
383.23	14.979	322.37
383.24	19.982	464.64
383.24	24.984	567.99
383.24	29.986	638.80
388.23	10.023	178.45
388.23	14.988	308.26
388.23	19.984	443.95
388.23	24.985	547.91
388.24	29.990	620.89

Table II. (Continued)

T (K)	P (MPa)	ρ ($\text{kg} \cdot \text{m}^{-3}$)
393.23	10.023	173.25
393.23	15.006	296.05
393.23	19.986	425.13
393.24	24.979	528.66
393.24	29.988	603.21
398.23	10.023	168.46
398.23	14.981	284.26
398.23	19.980	407.87
398.23	24.983	510.44
398.23	29.986	586.19
403.23	10.023	164.10
403.23	14.980	274.26
403.23	19.981	392.27
403.23	24.983	493.15
403.23	29.987	569.67
408.22	10.008	159.84
408.22	14.981	265.14
408.22	19.983	377.95
408.22	24.982	476.91
408.22	29.988	553.91
413.22	10.024	156.28
413.22	14.980	256.92
413.22	19.982	364.89
413.22	24.982	461.63
413.22	29.988	538.66
418.21	10.023	152.74
418.21	14.978	249.37
418.21	19.981	352.96
418.21	24.985	447.24
418.21	29.985	524.05
423.21	10.023	149.43
423.21	14.980	242.39
423.21	19.982	342.00
423.21	24.984	433.89
423.21	29.987	510.05
428.21	10.023	146.27
428.21	14.979	236.05
428.21	19.982	331.86
428.21	24.985	421.26
428.21	29.984	496.72
433.20	10.023	143.33
433.21	15.006	230.41

Table II. (Continued)

T (K)	P (MPa)	ρ ($\text{kg} \cdot \text{m}^{-3}$)
433.21	19.981	322.34
433.21	24.983	409.41
433.21	29.987	483.97
438.20	10.023	140.50
438.20	14.980	224.52
438.21	19.981	313.67
438.21	24.984	398.38
438.21	29.985	471.83
443.20	10.023	137.83
443.20	14.980	219.33
443.21	19.983	305.53
443.21	24.983	387.90
443.21	29.985	460.40
448.20	10.023	135.33
448.20	14.980	214.43
448.20	19.984	297.93
448.20	24.983	378.15
448.20	29.984	449.44
453.20	10.023	132.94
453.20	14.981	209.88
453.20	19.983	290.83
453.20	24.985	368.92
453.20	29.985	438.92
458.19	10.024	130.64
458.20	14.981	205.51
458.20	19.982	284.17
458.20	24.985	360.22
458.20	29.989	429.04
463.19	10.023	128.48
463.19	14.980	201.48
463.19	19.983	277.94
463.20	24.982	352.15
463.20	29.983	419.66
468.19	10.023	126.35
468.20	15.010	197.94
468.20	20.000	272.22
468.20	24.994	344.46
468.20	29.985	410.65
473.20	10.023	124.35
473.20	14.979	193.95
473.20	19.983	266.42
473.20	24.983	337.02
473.20	29.983	402.11

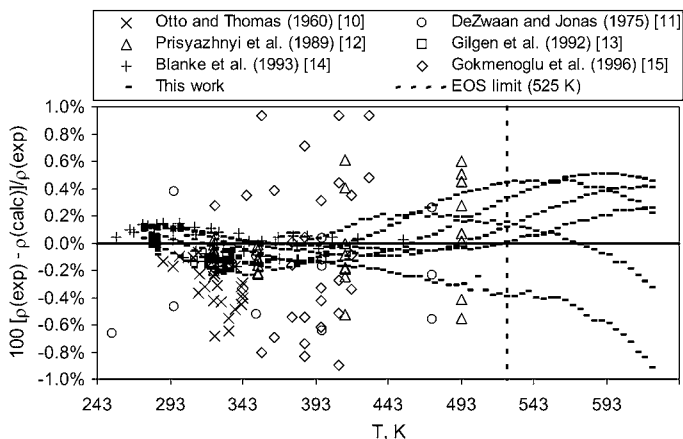


Fig. 5. Relative deviations between experimental densities at pressures up to 30 MPa and the equation of state for sulfur hexafluoride from de Reuck et al. [9] ($T_c = 318.7 \text{ K}$, $P_c = 3.76 \text{ MPa}$).

was limited, from 5 to 30 MPa. For a better illustration, the deviations in Fig. 5 are limited to $\pm 1\%$. The maximum temperature of the equation of state is marked as in Fig. 4. Some data of DeZwaan and Jonas [11] (maximum deviation of -3.8%) and Gokmenoglu et al. [15] (maximum deviation of $+8.9\%$) show larger deviations. Especially in the supercritical state ($T_c = 318.7 \text{ K}$ [1]), a larger scatter of the data is observed. It is somewhat surprising that the quality of the data does not depend on the

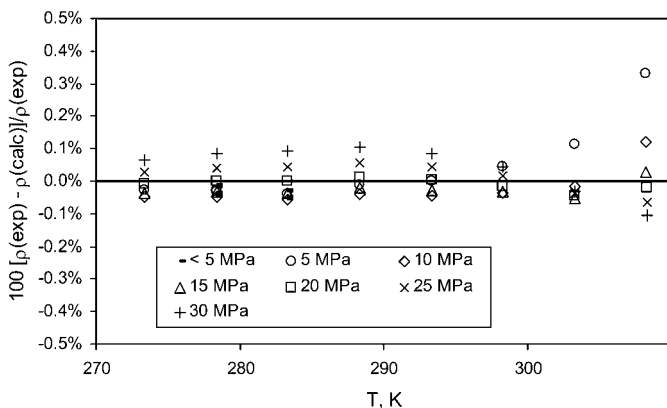


Fig. 6. Relative deviations between experimental densities and the TRIDEN correlation for sulfur hexafluoride ($T_c = 318.7 \text{ K}$, $P_c = 3.76 \text{ MPa}$).

year of publication. Our data are in good agreement with the high quality data of Gilgen et al. [13] and of Blanke et al. [14] and also with the highly scattered data of Otto and Thomas [10] and of Prisyazhnyi et al. [12]. On the other hand Gokmenoglu et al. [15] estimated an average uncertainty of $\pm 1.2\%$ for their density measurements. But the deviations indicate a questionable quality of their recent data.

For N_2O , only limited compressed density data [1] in the measured temperature and pressure range and no published equation of state are available for comparison. The measurements of Couch et al. [16] (from 243 to 423 K and up to 31 MPa), in the liquid state ($T_c = 309.6$ K [1]), agree very well with the new N_2O data (average mean deviation of 0.27%, between 273 and 309 K). Larger deviations are observed in the supercritical state for the values of Couch et al. [16] (0.72%, between 317 and 423 K) and the values from Schamp et al. [17] (3.3%, between 348 and 398 K up to 16.7 MPa). With the new measurements for N_2O the temperature range was extended up to 473 K and up to 40 MPa.

The measured $P\rho T$ data in the liquid phase for SF_6 and N_2O were correlated with the TRIDEN model. The complete set of densities in the sub- and supercritical regions for SF_6 and N_2O were correlated with a virial-type equation of state.

3.1. Correlation of Liquid $P\rho T$ Data with the TRIDEN Correlation System

For the correlation of the measured compressed liquid densities, the flexible $P\rho T$ correlation system TRIDEN was employed. TRIDEN stands for the three-dimensional (TRI) correlation of DENsities using the three well known equations from Tait for compressed densities [5], from Rackett for saturated densities [18], and from Wagner for vapor pressures [19].

The widely used Tait equation for isothermal compressed densities was combined with a modified Rackett equation (4) for the liquid saturation densities and the Wagner vapor pressure equation in the "2.5,5" form Eq. (5), used as a reference state (ρ_0 and P_0) which is required for the Tait equation [Eq. (6)]. The Rackett equation used here is a further modification of the modified form suggested by Spencer and Danner [18]. In this Rackett equation all four parameters can be simultaneously fitted to temperature-dependent experimental density data.

With the TRIDEN correlation program the temperature dependent parameters of the Tait equation can be fitted to isothermal densities (as measured in this work). With the help of these parameters the saturation densities can be obtained for each temperature by extrapolation. The required saturation pressures are calculated with the Wagner equation using our correlation parameters of DDB-Pure. These parameters were

fitted with evaluated experimental vapor pressure data from different researchers [1]. The saturation densities are then correlated with the Rackett equation. For nonisothermal density data (mainly stored in the DDB pure component data bank), the Rackett parameters are fitted to experimental saturation densities.

The modified Rackett equation for saturation density ρ_0 (in $\text{kg} \cdot \text{m}^{-3}$) is as follows:

$$\rho_0 = A_R / B_R^{[1+(1-(T/C_R))^{D_R}]} \quad (4)$$

The Wagner equation for vapor pressure P_0 (in MPa) is expressed as

$$\ln(P_0) = \ln(P_c) + \frac{A_W(1-T_r) + B_W(1-T_r)^{1.5} + C_W(1-T_r)^{2.5} + D_W(1-T_r)^5}{T_r} \quad (5)$$

The Tait equation for isothermal compressed densities ρ (in $\text{kg} \cdot \text{m}^{-3}$) is given by:

$$\rho = \rho_0 \left/ \left[1 - C_T \ln \left(\frac{B_T + P}{B_T + P_0} \right) \right] \right. \quad (6)$$

where the following temperature dependence is used for the parameter B_T :

$$B_T = b_0 + b_1 \frac{T}{E} + b_2 \left(\frac{T}{E} \right)^2 + b_3 \left(\frac{T}{E} \right)^3$$

and for the parameter C_T , a linear temperature dependence is used:

$$C_T = c_0 + c_1 \left(\frac{T}{E} \right)$$

The flexibility of combining different independent equations (for compression, saturation density, and vapor pressure), the adaptability of the number of parameters for the temperature dependence of the Tait parameters B_T and C_T (e.g., C_T may be assumed as a constant for a narrow temperature range), and the possibility of a reliable pressure and temperature extrapolation are the main advantages of this approach. In this case for the quite narrow temperature range of the measured liquid phases of SF_6 and N_2O , the parameter C_T was fitted as a constant. Furthermore the equations for the saturation density (e.g., polynomial of T_r) or the vapor pressure (e.g., Antoine equation) can be easily exchanged. If no vapor

pressure equation is available or applicable, the reference pressure may be set to a constant value, e.g., 1 MPa and the reference density equation describes densities at this pressure. Below the normal boiling point the reference pressure is always 0.1013 MPa if a vapor pressure equation is employed.

Using these equations it is possible to correlate the $P\rho T$ data in the whole liquid state up to the critical point, nearly within experimental error. With the developed TRIDEN Excel-Add-In, further properties, e.g., isothermal compressibility, thermal expansion coefficient, or the pressure dependence of the molar heat capacity, can be calculated as well.

Besides a deviation plot other statistical values are desirable to evaluate the correlation. The absolute, RMSD [Eq. (7)], and relative, RMSDr [Eq. (8)], root-mean-square deviations, and the mean deviation, bias [Eq. (9)], are utilized as statistical measures of the TRIDEN fits.

$$\text{RMSD} = \sqrt{\frac{1}{n} \sum_n (\rho_{\text{exp}} - \rho_{\text{calc}})^2} \quad (\text{kg} \cdot \text{m}^{-3}) \quad (7)$$

$$\text{RMSDr} = 100 \sqrt{\frac{1}{n} \sum_n \left(\frac{\rho_{\text{exp}} - \rho_{\text{calc}}}{\rho_{\text{exp}}} \right)^2} \quad (\%) \quad (8)$$

$$\text{bias} = \frac{1}{n} \sum_n (\rho_{\text{exp}} - \rho_{\text{calc}}) \quad (\text{kg} \cdot \text{m}^{-3}) \quad (9)$$

The relative root-mean-square deviation between the DDB-Pure correlation (from literature values of different researchers) for saturated liquid densities of sulfur hexafluoride and the calculation with TRIDEN (extrapolation to the saturation pressure) is 0.27% between 273 and 308 K.

The TRIDEN parameters for the Tait equation, the Rackett equation, and the Wagner equation, the temperature and pressure ranges covered and additional statistical values are given in Table III. The units are K, MPa and $\text{kg} \cdot \text{m}^{-3}$ with the exception of the critical pressure for the Wagner equation which is given in kPa.

For a larger range of applicability, all liquid density data were fitted together, except for the density data measured between $T_c - 10$ K up to the critical temperature T_c . These data were omitted from the fitting procedure because of the larger experimental errors near the critical point. In Figs. 6 and 7 the relative deviations between experimental values and the correlation are shown. For sulfur hexafluoride and dinitrogen monoxide the deviations are usually within ± 0.1 and $\pm 0.2\%$, respectively. These deviations are somewhat higher than the estimated experimental uncertainties but within the normal scatter of precise density measurements from different

Table III. Parameters for the TRIDEN Correlation Model for Sulfur Hexafluoride and Dinitrogen Monoxide (Temperature Range, Pressure Range, Number of Data Points, Tait Parameters, Rackett Parameters, Wagner Parameters, Critical Temperature, Critical Pressure and Absolute, RMSD, and Relative, RMSDr, Root-Mean-Square Deviations, and the Mean Deviation, Bias as Statistical Values for the TRIDEN Fit. Units: K, MPa, and $\text{kg} \cdot \text{m}^{-3}$)

	Sulfur hexafluoride	Dinitrogen monoxide
T_{\min} (K)	273.4	273.4
T_{\max} (K)	308.3	303.3
P_{\min} (MPa)	2.95	5.98
P_{\max} (MPa)	29.99	40.02
ρ_{\min} ($\text{kg} \cdot \text{m}^{-3}$)	1329.2	739.7
ρ_{\max} ($\text{kg} \cdot \text{m}^{-3}$)	1778.5	1051.1
data points	64	79
c_0 (Tait)	0.079988	0.081674
c_1 (Tait)	0	0
b_0 (Tait)	175.0349	283.4875
b_1 (Tait)	-74.02396	-141.225
b_2 (Tait)	-2.23761	7.95502
b_3 (Tait)	2.47163	2.36645
E (Tait)	100	100
A (Rackett)	162.88186	101.86879
B (Rackett)	0.24876623	0.24951733
C (Rackett)	319.07089	307.99728
D (Rackett)	0.24390195	0.25485053
RMSD	0.9639	1.1158
RMSDr	0.0642	0.1261
bias	-0.0785	-0.0856
A (Wagner)	-7.3512301	-6.793613
B (Wagner)	2.4716001	1.5419191
C (Wagner)	-2.4716001	-1.5419191
D (Wagner)	-19.88028	-5.3063073
T_c (K)	318.7	309.6
P_c (kPa)	3760.2	7244.74

researchers. Near the critical temperatures larger, deviations are observed in all cases.

3.2. Correlation of Liquid and Supercritical $P\rho T$ Data with an Equation of State

A virial-type equation of state (10) was employed for the correlation of the complete $P\rho T$ data set of sulfur hexafluoride and dinitrogen monoxide in the sub- and supercritical states. The equation is a reduced version of the Benedict–Webb–Rubin-type Bender equation of state [20]. In this equation

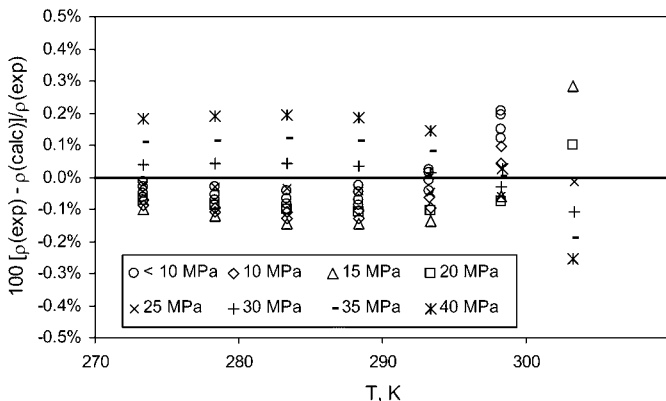


Fig. 7. Relative deviations between experimental densities and the TRIDEN correlation for dinitrogen monoxide ($T_c = 309.6$ K, $P_c = 7.24$ MPa).

the exponential term of the Bender equation was omitted. This means the number of parameters was reduced from 20 to 13.

The virial-type equation of state is

$$P = T\rho[R + B\rho + C\rho^2 + D\rho^3 + E\rho^4 + F\rho^5] \quad (10)$$

with the temperature dependent functions:

$$B = a_1 - \frac{a_2}{T} - \frac{a_3}{T^2} - \frac{a_4}{T^3} - \frac{a_5}{T^4}, \quad C = a_6 + \frac{a_7}{T} + \frac{a_8}{T^2}$$

$$D = a_9 + \frac{a_{10}}{T}, \quad E = a_{11} + \frac{a_{12}}{T}, \quad \text{and} \quad F = \frac{a_{13}}{T}$$

with the general gas constant $R = 0.008314472$ (MPa · L · mol⁻¹ · K⁻¹) and the molar density ρ (in mol · L⁻¹).

The data were correlated by least-squares minimization using the following objective function (11).

$$S = \sum_i [(\rho_{i, \text{exp}} - \rho_{i, \text{calc}}) / \rho_{i, \text{exp}}]^2 \quad (11)$$

Table IV gives the 13 parameters of the equation of state together with additional statistical values. The absolute, RMSD, and relative, RMSDr, root-mean-square deviations, and the mean deviation, bias, were calculated for the density and for the pressure. The units are K, MPa, and mol · L⁻¹.

Table IV. Parameters for the Virial Equation for Sulfur Hexafluoride and Dinitrogen Monoxide (Temperature Range, Pressure Range, Number of Data Points, Equation of State Parameters and Absolute, RMSD, and Relative, RMSDr, Root Mean Square Deviations, and the Mean Deviation, Bias of Density and Pressure as Statistical Values for the Fit. Units: K, MPa, and mol · L⁻¹)

	Sulfur Hexafluoride	Dinitrogen Monoxide
T_{\min} (K)	273	273
T_{\max} (K)	623	473
P_{\min} (MPa)	3	6
P_{\max} (MPa)	30	40
ρ_{\min} (mol · L ⁻¹)	0.978	2.825
ρ_{\max} (mol · L ⁻¹)	12.178	23.882
data points	442	251
a_1	0.00097909	0.00029673
a_2	0.51607005	0.1018373
a_3	115.98519	104.85244
a_4	-1056.1583	-5313.0187
a_5	229.28465	-192.00369
a_6	0.00020853	3.96838E-05
a_7	-0.13884117	-0.02358371
a_8	21.272656	5.4308599
a_9	-3.4174E-05	-3.36039E-06
a_{10}	0.02947575	0.00230486
a_{11}	4.49992E-06	2.40324E-07
a_{12}	-0.00422928	-0.0001837
a_{13}	0.000143155	2.93143E-06
RMSD (density)	0.00844	0.01421
RMSDr (density)	0.12001	0.08999
bias (density)	-0.000104	-0.000345
RMSD (pressure)	0.11778	0.1142
RMSDr (pressure)	1.0906	0.7085
bias (pressure)	0.013158	0.01587

In Figs. 8 and 9 the relative deviations between the experimental and the correlated values are shown. For sulfur hexafluoride and dinitrogen monoxide, the deviations are usually within $\pm 0.2\%$. As expected near the critical temperature, larger deviations are observed for both fluids. In the supercritical state the deviations between the experimental values and the correlation are within the estimated experimental uncertainties. Considering a larger range of applicability, all measured density data were fitted simultaneously. Therefore, larger deviations are obtained in the liquid phase with the equations of state than with the TRIDEN correlations. It is furthermore recommended to use the equation parameters only within the temperature, pressure, and density ranges covered by the correlation and only for the calculation of $P\rho T$ properties.

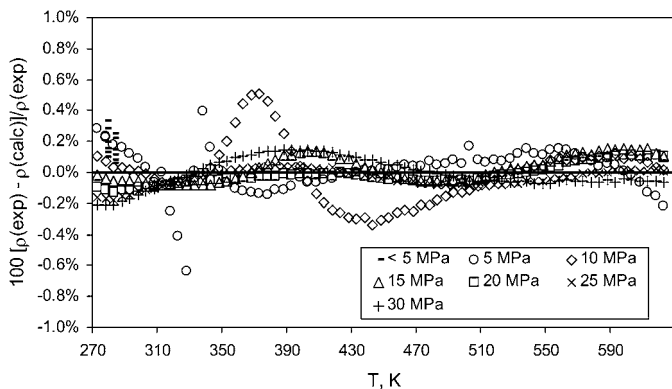


Fig. 8. Relative deviations between experimental densities and the equation-of-state correlation for sulfur hexafluoride ($T_c = 318.7$ K, $P_c = 3.76$ MPa).

For sulfur hexafluoride the isothermal compressibilities (12) calculated with the equation of state (10) were compared with the results obtained using the reference equation of state by de Reuck et al. [9].

$$\chi = -\frac{1}{v} \left(\frac{\partial v}{\partial P} \right)_T \quad (12)$$

The result was a tolerable relative root-mean-square deviation of 2.02% in the supercritical range and 3.23% for the complete temperature and pressure range with a maximum relative deviation of 16.2% near the critical point.

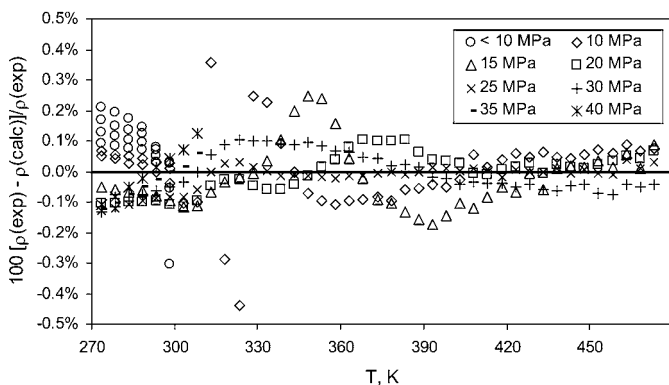


Fig. 9. Relative deviations between experimental densities and the equation-of-state correlation for dinitrogen monoxide ($T_c = 309.6$ K, $P_c = 7.24$ MPa).

4. SUMMARY AND OUTLOOK

For the measurement of liquid densities and densities in the compressed supercritical state up to 623 K and 40 MPa, a new computer-controlled high-temperature, high-pressure vibrating tube densimeter was employed [4]. Up to now vibrating tube densimeters have not been used for measurements in the supercritical state. The density measurements are fully automated using defined temperature-pressure programs. With respect to accuracy, reliability, suitability, and time consumption this system represents an optimum for measuring $P\rho T$ properties.

Compressed liquid densities and compressed supercritical densities of sulfur hexafluoride (SF_6) and dinitrogen monoxide (N_2O) were measured and correlated. Up to now, no density data for SF_6 and N_2O covering this wide temperature and pressure range were published. For the correlation of compressed liquid densities for SF_6 and N_2O , the new correlation system TRIDEN (a combination of well known equations) was applied.

The density measurements for SF_6 and N_2O are a continuation of the density measurements performed for toluene, carbon dioxide, carbonyl sulfide, and hydrogen sulfide [4]. For the improvement and development of new Helmholtz-type equations of state for toluene, H_2S , and COS [21] and N_2O [21, 22], the measured densities will be used. The densities of SF_6 could be used to extend the temperature range of the IUPAC interim reference equation of state. In the future, densities in the compressed liquid phase for some ethers and other compounds will be published. Furthermore, measurements on compressed liquid densities for binary mixtures will be presented. This should demonstrate the suitability of the measurement system for measuring densities of mixtures, i.e., excess volumes depending on temperature and pressure.

ACKNOWLEDGMENT

The authors would like to thank the "Labor für Meßtechnik Dr. Hans Stabinger" (Graz, Austria) for supplying the DMA-HDT prototype and the "Max Buchner-Forschungstiftung" for financial support of this work.

SUPPLEMENT

Supporting Information Available: The mentioned TRIDEN Excel-Add-In (for Excel 97 or higher) can be obtained from the authors.

REFERENCES

1. Dortmund Data Bank for Pure Component Properties (DDB-Pure), DDBST GmbH, www.ddbst.de (Oldenburg, Germany, 2002).

2. O. Kratky, H. Leopold, and H. Stabinger, *Z. Angew. Phys.* **27**:273 (1969).
3. E. C. Ihmels, C. Aufderhaar, J. Rarey, and J. Gmehling, *Chem. Eng. Technol.* **23**:409 (2000).
4. E. C. Ihmels and J. Gmehling, *Ind. Eng. Chem. Res.* **40**:4470 (2001).
5. J. H. Dymond and R. Malhotra, *Int. J. Thermophys.* **9**:941 (1988).
6. A. Pruß and W. Wagner, *The 1995 IAPWS—Formulation for the Thermodynamic Properties of Ordinary Water Substance for General and Scientific Use*, personal communication as windows-dynamic link library (Ruhr Universität, Bochum, Germany, 1998).
7. K. Watanabe and R. B. Dooley, *The International Association for the Properties of Water and Steam, Release on the IAPWS Formulation 1995 for the Thermodynamic Properties of Ordinary Water Substance for General and Scientific Use* (www.iawps.org) (Fredericia, Denmark, 1996).
8. B. A. Younglove and J. F. Ely, *J. Phys. Chem. Ref. Data* **16**:577 (1987).
9. K. M. de Reuck, R. J. B. Craven, and W. A. Cole, *Report on the Development of an Equation of State for Sulphur Hexafluoride*, IUPAC Thermodynamics Tables Project Centre Rep. PC/D 44 (London, United Kingdom, 1991).
10. J. Otto and W. Thomas, *Z. Phys. Chem., Neue Folge* **23**:84 (1960).
11. J. DeZwaan and J. Jonas, *J. Chem. Phys.* **63**:4606 (1975).
12. A. P. Prisyazhnyi, E. E. Totskii, and E. E. Ustyayhnin, *Teplofiz. Vys. Temp.* **27**:400 (1989).
13. R. Gilgen, R. Kleinrahm, and W. Wagner, *J. Chem. Thermodyn.* **24**:953 (1992).
14. W. Blanke, G. Kligenberg, and R. Weiß, *PTB-Mitteilungen* **103**:27 (1993).
15. Z. Gokmenoglu, Y. Xiong, and E. Kiran, *J. Chem. Eng. Data* **41**:354 (1996).
16. E. J. Couch, K. A. Kobe, and L. J. Hirth, *J. Chem. Eng. Data* **6**:229 (1961).
17. H. W. Schamp, E. A. Mason, and K. Su, *Phys. Fluids* **5**:769 (1962).
18. C. F. Spencer and R. P. Danner, *J. Chem. Eng. Data* **17**:236 (1972).
19. D. Ambrose, *J. Chem. Thermodyn.* **18**:45 (1986).
20. E. Bender, *Cryogenics* **15**:667 (1975).
21. E. W. Lemmon, personal communication (National Institute of Standards and Technology, Boulder, Colorado, U.S.A., 2002).
22. C. Bonsen, personal communication (Ruhr-Universität Bochum, Bochum, Germany, 2002).